# Fluctuating Arctic sea ice thickness changes estimated by an in-situ learned and empirically forced neural network model

G. I. Belchansky[1], D. C. Douglas[2*], N. G. Platonov[1]

[1] Space Monitoring & Ecoinformation Systems Sector
Institute of Ecology, Russian Academy of Sciences
Leninsky Prospect 33, Moscow, Russia 119071
Phone: (495) 135-9725; Fax: (495) 135-9972
E-mail: belchans@eimb.ru

[2] U.S. Geological Survey Alaska Science Center
Juneau Field Station
3100 National Park Road, Juneau, AK, USA 99801
Phone: (907) 364-1576; Fax: (907) 364-1540
E-mail: ddouglas@usgs.gov

*Journal of Climate*
June 20, 2007

[*] Corresponding Author

**Abstract**

Sea ice thickness (SIT) is a key parameter of scientific interest because understanding the natural spatiotemporal variability of ice thickness is critical for improving global climate models. In this paper, we examine changes in Arctic SIT during 1982–2003 using a neural network (NN) algorithm trained with in situ submarine ice draft and surface drilling data. For each month of the study period, the NN individually estimated SIT of each ice-covered pixel (25-km resolution) based on 7 geophysical parameters (4 shortwave and longwave radiative fluxes, surface air temperature, ice drift velocity, and ice divergence/convergence) that were cumulatively summed at each monthly position along the pixel's previous 3-year drift track (or less if the ice was <3 years old). Average January SIT increased during 1982–88 in most regions of the Arctic (+7.6 ± 0.9 cm $yr^{-1}$), decreased through 1996 Arctic-wide (-6.1 ± 1.2 cm $yr^{-1}$), then modestly increased through 2003 mostly in the central Arctic (+2.1 ± 0.6 cm $yr^{-1}$). Net ice volume change in the Arctic Ocean from 1982 to 2003 was negligible, indicating that cumulative ice growth had largely replaced the estimated 45000 $km^3$ of ice lost by cumulative export. Above 65° N, total annual ice volume and interannual volume changes were correlated with the Arctic Oscillation (AO) at decadal and annual time scales, respectively. Late-summer ice thickness and total volume varied proportionally until the mid-1990s, but volume did not increase commensurate with the thickening during 1996–2002. The authors speculate that decoupling of the ice thickness-volume relationship resulted from two opposing mechanisms with different latitudinal expressions: a recent quasi-decadal shift in atmospheric circulation patterns associated with the AO's neutral state facilitated ice thickening at high latitudes while anomalously warm thermal forcing thinned and melted the ice cap at its periphery.

## 1. Introduction

At present, distinguishing between natural and human-induced climate change is an overarching challenge among global climate studies (Hansen et al. 2006). The problem is often addressed using climate models that are premised on general circulation theories of the ocean and atmosphere. The climate models require in situ experiments to provide both a foundation and parameterization of the underlying dynamic physical processes that govern the climate system. Sea ice thickness (SIT) is a key variable in the Arctic climate system, and thickness distributions play an important role in regional and global climate prediction (Rind 1995; Walsh et al. 2002). Rates of heat transfer between the ocean and the atmosphere, as well as rates of ice production and melt, are closely related to SIT distributions (Deser et al. 2000). Surface heating and evaporation rates affect stratification, cloudiness, and circulation of the lower atmosphere, while the rates of ice melt and freeze influence fresh water fluxes that affect ocean stratification and circulation (Deser et al. 2002; Polyakov et al. 2002; Boyd et al. 2002). One of the primary sources of uncertainty in global climate models is thought to lie in their assorted and rudimentary representations of sea ice (Holland and Bitz 2003), although significant improvements have been made in recent years (Holland et al. 2006).

Studies indicate that climate sensitivity depends more on SIT than on ice extent, and that biases in the simulation of sea ice arise from uncertainties in the parameterization of surface fluxes and oversimplified treatment of lateral freezing and melt (Parkinson et al. 2001; Winsor 2001; Steele et al. 2001). Uncertainties among models can also arise from differences in the methods used to couple the ocean, ice, and atmosphere processes (Walsh et al. 2002), making it complicated to determine whether SIT is controlled mainly by changes in thermodynamic or dynamic forcing (Zhang et al. 2000). Overall, to improve the treatment of sea ice thickness in

climate simulation and prediction, more accurate data are needed about the Arctic's SIT distributions in conjunction with more detailed analyses (Walsh et al. 2002; Holland and Bitz 2003, Bitz and Roe 2004).

Sea ice thickness changes have been aggressively investigated in recent years using sophisticated coupled ice-ocean models (Zhang et al. 2000; Lindsay and Zhang 2005), satellite altimetry (Laxon et al. 2003), and a variety of in situ measurement technologies such as upward looking sonar (Vinje et al. 1998; Rothrock et al. 1999; Winsor 2001; Widell et al. 2003) and electromagnetic profiling (Haas and Eicken 2001; Eicken et al. 2001). Still, differences among model results are testimony to their uncertainty (Holland and Bitz 2003), and ice dynamics complicate broad-scale extrapolations of sparsely sampled in situ SIT measurements (Holloway and Sou 2002; Rothrock et al. 2003). At present, sea ice thickness remains an important yet difficult parameter to estimate Arctic-wide (Miller et al. 2006).

In this paper we examine spatiotemporal SIT dynamics with a distinctly novel methodology that uses a neural network (NN) to empirically estimate and emulate the complex relationships among several forcing parameters. We describe how the NN was constructed and learned, and compare the NN estimates to several published studies that obtained SIT from field measurements or modeling. We then examine how apparent periods of increasing and decreasing SIT translated to ice volume changes, and how those changes may have been affected by changes in atmospheric circulation patterns and thermal forcing.

We show that although the satellite and other data records are relative short, they capture a pronounced period of change in sea ice and atmospheric dynamics and hence contain useful information for extracting an improved understanding of the mechanisms responsible for recent SIT changes in the Arctic. While our study complements the work done by others by

contributing a new approach and interpretation of SIT changes during the past two decades, all retrospective hemispheric-scale SIT models possess uncertainty because their validation is precluded by an intrinsic lack of sufficient historical data.

## 2. Methods

We hypothesized that for any parcel (or pixel) of ice-covered ocean, its principal monthly SIT change results from an integration of the main geophysical forcing mechanisms that control energy exchanges across the ocean-ice-atmosphere boundaries during that month. Thus, if a pixel of ice is followed for several months (or years) of drift, its net SIT change will be manifest through an accumulation of the geophysical forcing at each position along its drift trajectory. In general, our methodological approach was to use a NN to estimate SIT at 25 km x 25 km resolution (one pixel) based on a set of accumulated (integrated over time) geophysical forcing parameters from each monthly location during several years of prior ice drift. To initially construct the NN by a learning process, we accumulated the forcing parameters for pixels with known SIT based on submarine upward looking sonar and ice coring measurements. Details are presented below.

Several in situ and quasi-observational environmental data sets were assimilated for constructing the NN: sea ice concentrations from the SMMR-SSM/I (Comiso 1999), monthly mean ice motion vectors from satellite observations (Fowler 2003), surface air temperatures (SAT) from the IABP/POLES (Rigor et al. 2000), and atmospheric and radiative flux estimates from the NCEP-NCAR Reanalysis (http://www.cdc.noaa.gov). The SAT and NCEP data were interpolated to 25-km resolution and projected to the SSM/I polar stereographic grid. Submarine upward-looking sonar (SULS) ice draft profiles (NSIDC 1998) and ice coring data from aircraft

landing observations (ALO) (NSIDC 2004) were used for the NN learning and 'validation', and data from SULS cruises that were declassified and made available in 2006 were used for 'testing' (sensu Bishop 1995).

Learning data for the NN were prepared from SULS transect segments by assigning the median sea ice draft to the segment's midpoint location. The SULS point data were rasterized by month within year (averaged if >1 point per pixel) to the polar stereographic 25-km grid, multiplied by 1.12 to include free-board thickness (Rothrock et al. 1999), and smoothed with a 5 x 5 low-pass filter. The learning data from ALO drill holes used SIT of the prevailing ice type (without correction for hummocking), and were gridded and smoothed as above. Smoothing was performed to help achieve a spatial resolution more commensurate with the NCEP and SAT data, and imposed little change to the original SIT values ($\rho = 0.96$).

We chose the median SULS statistic instead of the mean to reduce the influences of extremely thick drafts that occasionally occurred, and to attain closer correspondence with ALO measurements of the prevailing (presumably modal) ice type. Owing to the network's coarse spatial and temporal resolution, we had no expectation for it to possess local-scale sensitivity to processes associated with the formation of extremely thick ice ridges. Among 2157 25-km-square pixels, a high degree of correlation between the mean and median ice draft ($\rho = 0.97$), the mean and mode ($\rho = 0.85$), and the median and mode ($\rho = 0.91$), support our implicit assumption that within-pixel SIT variation is generally isotropic and adequately represented (for purposes of this study) by a linear SULS transect.

We started with 22 parameters known to influence SIT, including estimates of various short and longwave irradiances and net fluxes, atmospheric pressure, wind speed, relative humidity, SAT, ice concentration, ice drift velocity, and an ice divergence/convergence index

(D/C). The monthly D/C index was calculated by advecting a uniform distribution of points (25-km pixel centers) with the respective month's ice motion vectors, summing the resultant points within the boundaries of each 25-km pixel, and smoothing. Although insensitive to fine-scale ice dynamics, D/C values near zero generally indicate divergent ice conditions, while values >1 infer increasing convergence.

For each learning data pixel (n = 2157 SULS; n = 907 ALO), the 22 parameters were cumulatively summed at each monthly location as the pixel's drift was followed in reverse chronology during its lifetime, or until reaching a threshold of maximum accumulated time. A pixel's back-trajectory was derived using a reverse chronology algorithm that tracked each ice-covered pixel to its location and date of origin, based on monthly ice motion data and monthly sea ice masks (Belchansky et al. 2005a). The trajectory established lifetime (age) and origin of the ice by determining when and where the pixel originally changed from water (<15% ice concentration) to ice (≥15%). Three different data sets were constructed based on three thresholds of maximum accumulated time: 36, 60, and 84 months.

Estimating high-order nonlinear relationships requires a NN to possess complex internal structure. The upper limit of complexity is determined by learning data volume, so it was advantageous to reduce the number of input parameters. We used stepwise regression analyses and preliminary network trials to select 7 of the 22 parameters for the final NN: 1) freeze degree-month, defined as departure (°C) of the monthly mean SAT below –2°C (or 0 for months with mean SAT ≥ –2°C); 2) ice drift velocity (cm $s^{-1}$); 3) the ice D/C index ($mo^{-1}$); and surface-level monthly means (W $m^{-2}$) of 4) clear sky downward solar flux; 5) clear sky downward longwave flux; 6) net shortwave radiation flux; and 7) net longwave radiation flux.

Trial and error tests indicated that a three-layer perceptron without shortcut connections and 7-12-1 topology optimized the network's complexity, computational efficiency, and ability to simulate the learning data. Hidden neurons had logistic (sigmoid) activation functions, while input and output neurons had 'identity' activation functions. That is, input neurons passed their input values to hidden neurons without change, so the output of the output neuron was the weighted sum of its inputs and bias. We used a resilient propagation algorithm for the learning process to restrain over-fitting of the learning data (Riedmiller and Braun 1993).

A NN was constructed by randomly splitting the learning data, using one half for learning and the other half for validation. Ten NNs were constructed in this manner. We found that accumulating the 7 input parameters >36 months did not significantly improve the network's simulation of the learning data. Consequently, each final monthly SIT map was independently created, one pixel at a time, by accumulating the 7 geophysical parameters along the monthly drift track of each ice-covered pixel during its previous 36-month history (or less if the ice was <36 months old), then using the 7 sums as the inputs to each of the 10 NNs, and then averaging the 10 SIT estimates. Availability of sea ice motion data limited our production of monthly SIT maps to January 1982 through March 2003.

## 3. Neural Network Assessment

We validated the NN by comparing its SIT estimates to the original learning data, and we also tested the NN SIT estimates by comparing them to SULS data that were independent of the network's derivation. Mean discrepancy between the NN SIT estimates and the learning data (n = 3064 pixels) was near zero, with a 0.5 m rms. Across years, seasons, and latitude, the NN SIT estimates were similar to the learning data, but always less variable (Figs. 1a–c). The NN likely

underestimated the local-scale SULS SIT variability because the network was: 1) constructed using learning data from several years and seasons in a single combined analysis, 2) forced by relatively coarse resolution inputs, and 3) less inclined to simulate the noise component of the SULS measurements. Pooling all learning data improved the NN's robustness to estimate monthly SIT Arctic-wide, but likely compromised its sensitivity to simulate the magnitude of local SIT variability and the seasonal amplitude local SIT change.

We used data from 13 recently (2006) declassified SULS cruises to independently test the NN's accuracy (Figs. 1d–f). The overall mean difference (SULS minus NN) was +0.02 m (0.72 m rms, n = 844 pixels), with the NN explaining 48% of the SULS variability ($\rho = 0.69$). These comparisons provide the most robust evaluation of the NN's performance. Overall, the 0.72 m rms discrepancy and the 0.69 correlation between the NN SIT estimates and the independent in situ SIT measurements were very similar to those of other SIT model validations (Rothrock et al. 2003; Zhang et al. 2003).

We also compared the NN SIT estimates to several published studies that measured ice thickness at a variety of temporal and spatial scales (Table 1). We compared single NN SIT pixels to studies that measured ice thickness once at site-specific locations. For studies that summarized ice thickness within regions, across transects, or time-integrated monitoring stations, we attempted to ameliorate scale-related sampling incongruities by averaging the NN SIT estimates over commensurate areas and periods. Nevertheless, irresolvable space-time sampling disparities warrant judicious interpretation of the comparisons in Table 1.

Across all studies compared, no consistent biases were evident (Table 1). We expected similarities with Rothrock et al. (1999) and Yu et al. (2004) because they also used SULS data, so we consider these comparisons to be non-independent. Among the independent studies, SIT

discrepancies generally averaged between ±0.5 m and the error variances were typically higher than the learning data rms. The most pronounced differences were at sites with unique physiographic (southeast Beaufort Sea) or ice motion (Fram Strait) characteristics. Comparisons across the Fram Strait transect (78.5°N, 16.0°W; 80.0°N, 12.5°E) used monthly SIT estimates derived from Vinje et al. (1998, Tables 5 and 9) and Kwok and Rothrock (1999, Tables 3a and 5a), calculated as the quotient of ice volume flux and ice area flux during October 1990 through May 1996. The mean NN SIT during this 68-month period was 2.54 ± 0.35 m, similar but less variable than the averages for Vinje et al. (2.56 ± 0.53 m) and Kwok and Rothrock (2.41 ± 0.99 m). The level of discrepancy between the Vinje et al. and Kwok and Rothrock studies themselves (mean = 0.15 m, rms = 0.81) was comparable to that of the NN (Table 1).

We also examined sensitivity of the NN SIT estimates to the pixel-tracking algorithm. Independently, we varied the 15% ice concentration threshold that defined open water from 10–50% (in 10% increments), we scaled the ice vector velocities by 0.9x and 1.1x, and we introduced random phase changes to the ice vector trajectories (uniform distribution, ± $\pi$/4). For computational efficiency, we constructed one-layer 7-parameter networks for each evaluation using linear least-squares learning (Castillo et al. 2002). Across all evaluations, mean SIT differences between the original NN and the networks derived from (and applied to) the adjusted data were < 0.04 m, with rms values < 0.15 m. Thus, the NN appeared robust to plausible errors in the ice motion data and to the 15% ice concentration threshold that defined open water. We attribute this robustness, in part, to the network's ability to make compensations for modest noise or biases in the input data during its learning process.

In summary, spatiotemporal sampling incongruities between in situ SIT measurements and the monthly 25-km-resolution NN model preclude definitive estimates of the network's

accuracy. By virtue of its construct, the NN produced a smoother spatial and temporal rendition of SIT than that measured at finer-scale in situ sample locations. Internally, however, relative SIT changes in the NN time series should possess reasonable comparative precision because: 1) the learning data were well distributed over the temporal and spatial domains of study; 2) no consistent biases were observed between the NN estimates and the testing data; and 3) each monthly SIT map was independently estimated.

## 4. Results and Discussion

*a. Thickness distributions and change*

Arctic-wide, the SIT maps derived with the NN methodology (Fig. 2a) were remarkably consistent with prevailing knowledge (Bourke and Garret 1987): the thickest ice occurred along the northern Canadian Archipelago where it is compressed by the Beaufort Gyre and Transpolar Drift Stream, and the thinnest ice occupied the peripheral seas (Beaufort, Chukchi, Laptev, Kara, and Barents Seas) that are dominated by ephemeral first-year ice. Magnitudes of the NN SIT estimates were also commensurate with reported values (Haas 2004): January SIT above 65°N averaged 2.0 ± 0.9 m (range 0.5 – 4.7 m) and September averaged 2.3 ± 0.8 m (range 0.5 – 4.4 m). Variability in mid-winter SIT (Fig. 2a) was highest in the southern Beaufort Sea and along the northern Barents, Kara, and Laptev Seas where regional ice dynamics likely facilitate high fluxes of different ice age classes.

The 22-year time-series did not possess a significant linear SIT trend after the degrees of freedom were adjusted to account for temporal autocorrelation (Santer et al. 2000). The time-series did, however, encompass a period of distinctly alternating SIT fluctuations (Fig. 2b). Average January SIT increased (+7.6 ± 0.9 cm $yr^{-1}$) in most regions until reaching a maximum in

1988 (2.8 m), then decreased (-6.1 ± 1.2 cm $yr^{-1}$) Arctic-wide to a minimum in 1996 (2.3 m), and then modestly increased (+2.1 ± 0.6 cm $yr^{-1}$) through 2003 primarily in the central basin.

For perennial sea ice, all months in the NN time-series possessed the same overall decadal-scale pattern of SIT fluctuation (Fig. 3a). In Fig. 3, SIT was quantified within a fixed region of persistent perennial ice cover (defined by the intersection of all 1982–2002 September ice extents) to remove the influence that seasonal first-year ice imparts on area-averaged thickness. The oscillating character of SIT change over the 22-year record (increasing in the 1980s, rapidly decreasing in the early 1990s, and stabilizing after the mid-1990s) is notably similar to several NCEP-forced models of Arctic sea ice volume (Hilmer and Lemke 2000; Fichefet et al. 2003; Köberle and Gerdes 2003; Rothrock and Zhang 2005) and thickness (Rothrock et al. 2003). Given the NN's very different methodological basis, its overall agreement with several conventional models affords a notable qualitative cross-validation. Since the conventional models also used NCEP data, biases or errors among mutual forcing parameters (Curry et al. 2002) might manifest a degree of artificial similarity among the model outputs. However, the NN method is largely resilient to this issue because biases or errors, if present, would be compensated during the network's learning process.

Annual amplitude of the SIT change in perennial ice averaged 0.46 ± 0.08 m (Fig. 3b). Near the pole (100 km radius) the SIT amplitude averaged 0.60 ± 0.15 m, with maximums typically occurring in March and minimums in August. The NN's SIT amplitude was slightly greater than Johannessen et al. (2004) who estimated an ~40 cm seasonal SIT change in perennial ice using surface elastic-gravity waves measured at Russian North Polar drifting stations during 1970–91, and less than Rothrock et al. (1999) who estimated an amplitude >1 m

based on a 40-year average of an NCEP-forced ice-ocean model with a 12-category ice thickness distribution (Zhang et al. 1998).

Around the North Pole (Fig. 4), the NN SIT estimates exhibited a pattern of fluctuation that was generally similar to the perennial ice overall (Fig. 3a) but with slightly greater decadal amplitude and greater seasonal variability. On average, SIT at the Pole increased and then decreased by ≈1.0 m during the first 10 years of study and then gradually increased ≈0.5 m over the next 10 years. In Fig. 4, we compare the NN SIT estimates to the mean, median, and mode of near-coincident SULS SIT measurements. All 3 SULS statistics portray a decreasing SIT period during the late 1980s and early 1990s, and all show an indication of slight thickening thereafter. Infrequent occurrences of extreme ice drafts inflated the SULS mean and variance compared to the median and mode. The NN, which was learned with median SULS and prevailing (presumably modal) ALO values, depicted SIT fluctuations that were more or less intermediate to the median and mode SIT measurements near the Pole, including the short time-series of NPEO data.

Laxon et al. (2003) investigated SIT changes for ice >1.0 m thick within 65.0° N – 81.5° N during 8 winters (1993–2001) using satellite altimetry measurements of ice freeboard elevation. Direct comparisons with Laxon et al. were confounded by our inability to completely exclude the influence of ice that was <1 m thick from the 25 km resolution NN SIT pixel estimates. Throughout the Eurasian shelf, Laxon et al. (2003, Fig. 1) depicted average winter SIT ranging between 2.0 – 2.5 m, but the NN estimates for this region rarely exceeded 2 m (Fig. 2a). We attribute most of this discrepancy to the fact that the NN was learned with median SIT values, which are typically less than mean SIT due to ridging (see Fig. 4), and to Laxon et al.'s reported +0.18 m bias in their mid-winter mean SIT estimates (due to their exclusion of thin ice).

Nevertheless, when we compared winter NN SIT anomalies below 81.5°N (or otherwise), including or excluding pixels with SIT <1 m, correlations with Laxon et al. were always insignificant, primarily because the NN did not detect thinning during 1999–2001. Although Hass (2004) also detected an SIT decline in summer 1998 based on electromagnetic profiles of 43 ice floes in the Transpolar Drift Stream, the SULS and ALO data do not corroborate a thinning tendency in either 1998 or 1999 (Figs. 1a and 4). Similar to Laxon et al., however, we did detect a significant correlation ($\rho$ = -0.57, S = 0.99, n = 21) between year-to-year changes in mid-winter (January) SIT and duration of the previous melt season (Belchansky et al. 2004a) over the Arctic Ocean.

*b. Volume fluctuations*

Here we examine ice volume changes in the Arctic Ocean, which we defined as the area encompassing water depths generally >50 m: i.e. a polygon mask covering the area north of Fram Strait, Spitsbergen, Franz Josef Land, North Land, New Siberian Islands, Wrangel Island, North America, and Greenland. Within this region ($\approx 5.70 \times 10^6$ km$^2$) we calculated the month-to-month ice volume change starting from January 1982, where monthly volume was the sum of all pixel volumes within the mask calculated as the product of their respective NN SIT estimate, ice concentration estimate, and pixel area. We also calculated monthly external ice volume flux by summing the volume of all pixels that moved into the study area (based on ice motion vectors) and subtracting the volume of all pixels that moved out of the study area. Results of these calculations are shown in Fig. 5.

Annually, ice volume increased during the winter with peak monthly accumulations reaching upwards of 1000 km$^3$ in the early winter (October and November) and commensurate

peak volume losses during in May and June (Fig. 5a). The seasonal oscillation of ice volume in the Arctic Ocean ranged from average lows that prevailed in August ($10.76 \pm 1.15\ 10^3$ km$^3$) to average highs that prevailed in March ($13.80 \pm 1.05\ 10^3$ km$^3$).

The fraction of monthly ice volume change in the Arctic Ocean due to ice advection (external flux) was almost always negative (Fig. 5a). Exports averaged 180 km$^3$ month$^{-1}$ and maximums reached upwards of 600 km$^3$ month$^{-1}$. During a 72-month period of overlap (August 1990 – July 1996), the NN average monthly volume loss ($214 \pm 125$ km$^3$ month$^{-1}$) was comparable but slightly less than Vinje et al.'s (1998) estimated average monthly volume export through the Fram Strait ($237 \pm 142$ km$^3$ month$^{-1}$), the primary site of ice advection from the Arctic Ocean.

During January 1982 – February 2003 (254 months), the cumulative external sea ice volume flux in the Arctic Ocean was $-44.8 \times 10^3$ km$^3$ (Fig. 5b). To maintain annual ice volume, more ice must form in the Arctic Ocean by freeze processes than is lost by melt; and to maintain salinity equilibrium, the volume of freshwater exported as ice must be compensated by terrestrial runoff and precipitation. Annual amplitude of the seasonal ice volume oscillation averaged $3.04 \pm 0.44\ 10^3$ km$^3$, with an increasing linear slope of $0.034 \pm 0.015\ 10^3$ km$^3$ yr$^{-1}$ (S = 97%). Beginning in 1982, ice volume in the Arctic Ocean increased approximately $2.2\ 10^3$ km$^3$ during the 1980s, decreased $3.1\ 10^3$ km$^3$ through the mid-1990s, and then increased $0.9\ 10^3$ km$^3$ through 2002 (Fig. 5b). Collectively, the net ice volume change from 1982 to 2003 was negligible, indicating that cumulative ice growth had mostly replaced the estimated 45000 km$^3$ of ice lost by cumulative export.

Over the 21-year study, monthly ice volume losses from June to July (labeled 'July' in Fig. 6) and from July to August increased linearly in the Arctic Ocean (Fig. 6). Conversely, the

volume of ice gained from November to December increased, and slight volume losses between March and April became neutral. Other months had insignificant linear slopes. Accelerating losses of summer ice volume are consistent with the well-documented decline in perennial ice extent (Comiso 2002; Belchansky et al. 2005b, Stroeve et al. 2005). Volume gain in December was inversely correlated with average SIT in both October ($\rho$ = -0.70, S > 0.99, n = 21) and November ($\rho$ = -0.76, S > 0.99, n = 21), reflecting the ability of thin ice to attain higher growth rates than thicker ice (Bitz and Roe 2004). These correlations were partly influenced by the amount of first-year (new) ice production. December volume gain was positively correlated with the area of open water in September ($\rho$ = 0.54, S = 0.99, n = 21). Larger areas of rapid new ice growth in October or November would tend to transfer more latent heat to the atmosphere, so a negative thermodynamic feedback (Holland et al. 2006) may have delayed the expression of compensatory volume gain until December.

*c. Thickness-volume relationships*

During late-winter 1982–2002 in the northern hemisphere (>65° N), ice thickness and volume were positively correlated ($\rho$ = 0.96, S > 0.99, n = 21) (Fig. 7a) because winter ice extent varied little (Parkinson and Cavalieri 2002) and we calculated volume as the product of ice area and mean SIT. That is, when area is constant, the ratio between mean thickness and total volume is constant. In contrast, late-summer ice cover (or perennial ice, sensu Comiso 2002) has varied considerably since it began a dramatic decline in the late 1980s. During the late summers of 1982–95, the thickness-volume relationship maintained positive correlation ($\rho$ = 0.78, S > 0.99, n = 14) (Fig. 7b). The ice thickened and thinned with fairly commensurate volume changes (Fig.

7c). But the thickness-volume relationship collapsed after 1996 ($\rho$ = -0.29, S = 0.53, n = 7) (Fig. 7b) when the ice began thickening without a corresponding volume increase (Fig. 7c).

We propose that decoupling of the ice thickness-volume relationship after 1996 was an expression of two opposing mechanisms: 1) a decadal scale shift in atmospheric circulation acting to restore the ice at higher latitudes; and 2) anomalously warm thermal forcing acting to erode the ice at southern latitudes. Timing of the mid-1990 SIT increase is congruent with purported decadal-scale oscillations (Polyakov and Johnson 2000) suggesting natural processes may have instituted a sea ice regime shift favoring ice accumulation. The recent thickening is also consistent with improved survival of older ice age-classes that began in the mid-1990s (Belchansky et al. 2005a). We speculate that the recent increase in SIT was more apparent at higher latitudes (Fig. 2b) because concurrent influxes of anomalously warm air (Comiso et al. 2003) and ocean water (Karcher et al. 2003; Polyakov et al. 2005; Woodgate et al. 2006), and increased downward longwave radiation fluxes (Francis and Hunter 2006) have made their most direct and opposing impact at the Arctic Ocean's periphery by retarding ice growth (Thorndike 1992), extending melt seasons (Stroeve et al. 2006) and promoting positive feedbacks (Lindsay and Zhang 2005; Serreze and Francis 2006).

During 1996–2002, the modest ice thickening in the central Arctic appears to have offset volume losses associated with a concurrent decline in late-summer ice extent. This relationship is unstable, however, because thickening cannot compensate volume indefinitely under conditions of declining ice extent. Data limitations prevented us from assessing how, or if, the 1996–2002 decoupled thickness-volume relationship may have changed during the most recent years (2003–06) of record-breaking summer ice retreat, but obviously a long-term extrapolation of the decoupled relationship (Fig. 7c) would be ill advised.

*d. Relationships with the Arctic Oscillation*

The three periods of alternating SIT change (Fig. 2b) coincide with dominant phases of atmospheric pressure and circulation characterized by the Arctic Oscillation (AO) index (Thompson and Wallace 1998). Relatively high-pressure conditions in the Arctic during the 1980s (low AO) facilitated ice thickening by maintaining colder SAT (Comiso 2003) and strengthening the Beaufort Gyre (Rigor et al. 2002). When the AO shifted to a high-index phase in the late 1980s, sea ice thickness began decreasing as cyclonic circulation anomalies brought longer melt seasons (Belchansky et al. 2004a) and accelerated export of the Arctic's oldest ice (Rigor and Wallace 2004). Since the mid-1990s, the AO has maintained a variably neutral state and SIT increased modestly despite persistently long melt seasons and record minimum extents.

Year-to-year changes in hemispheric (>65° N) ice volume were inversely correlated with the AO (Fig. 8). Annual changes in both minimum (Fig. 8a) and maximum (Fig. 8b) ice volume exhibited roughly the same linear relationship with the intervening wintertime (JFM) AO. Despite the ostensible paradox regarding weak relationships between the AO and several Arctic environmental parameters (Overland and Wang 2005), changes in annual sea ice volume maintained correlation with the AO even after the mid-1990s when the AO relaxed to a variably neutral phase. Considering that the NN inputs did not include an atmospheric pressure parameter per se, the strong and persistent relationship between annual ice volume changes and the AO affirms the influential role that atmospheric dynamics have played in governing the Arctic's sea ice balance (Rigor et al. 2002).

The yearly minimum total ice volume, however, was not correlated with concurrent AO conditions (Fig. 9). Rather, total ice volume in any given year was correlated with an

accumulation of the AO over several prior years, particularly at decadal scales. In contrast, annual volume changes had little relationship with the integrated past. Analogous correlations based on maximum annual ice volume (not shown) produced similar results to those in Fig. 9. Short-term atmospheric forces directly influence the short-term growth, melt, and export of ice, but total ice volume at any given time represents an accumulation of short-term changes over longer time periods. Hence, long-term volume changes tended to parallel the decadal phases of the AO. Sensitivity of this analysis was undoubtedly enhanced by the pronounced changes in atmospheric circulation patterns that occurred during the study period.

We extrapolated the linear relationship between the AO and the annual change in minimum ice volume (Fig. 8a) from 2003–06. The extrapolation estimated a net ice volume increase of 1000 $km^3$ over the four-year period owing to three consecutive negative AO winters in 2004–06. This volume increase equates to a seemingly plausible 0.18 m average SIT increase across the 2006 minimum ice extent of 5.7 x $10^6$ $km^2$ (NSIDC 2006). However, we are reluctant to endorse this predicted volume increase because recent environmental conditions in the Arctic may be well outside the domain of variability represented in the NN learning data – highlighting a deficiency among all neural networks in their ability to produce robust estimates when the input data extend beyond the network's sphere of learning (Belchansky et al. 2004b).

Of concern are four record-breaking years of minimum sea ice extent since 2002 (Stroeve et al. 2005; NSIDC 2006) that underscore the question about how long ice thickening can compensate volume losses under conditions of declining ice extent. Lindsay and Zhang (2005) concluded that the Arctic ice pack may have thinned and shrank to a point at which internal positive feedback mechanisms could dominate external forcing mechanisms in determining a trajectory of future change. Our reservation to extrapolate the relationship between ice volume

and the AO (Fig. 8a) lies in the fact that the NN was learned with data from a period when external forcing predominated.

We assume the NN results are robust through 2002, and speculate that external forcing associated with a recently relaxed AO modestly thickened the ice without increasing its total volume because opposing thermal anomalies were pronounced at the Arctic periphery where a battle over an equilibrium tipping point (Lindsay and Zhang 2005) is presently being waged. Retreat of the thermal encroachment and subsequent restoration of the ice pack would likely require a sustained period of high atmospheric pressure anomalies (a low-index AO); however some studies suggest this scenario to be unlikely under a regime of global warming (Shindell et al. 1999; Rind et al. 2001).

## 5. Conclusions

Sea ice thickness plays an important role in the Earth's climate system and is an influential parameter in global climate models because it modulates ocean-atmosphere energy exchanges over very large areas. But SIT remains a challenging parameter to estimate Arctic-wide. Here we have developed a unique methodology for estimating SIT that uses an empirically learned NN algorithm to emulate the complex relationships among principal forcing mechanisms. Despite its unorthodox approach, the NN produced results that were remarkably similar to those of several conventional models and with the general prevailing knowledge of sea ice thickness distributions in the Arctic.

The 1982–2003 time series of NN-derived monthly SIT estimates indicated three alternating periods of change. The three periods aligned with dominant phases of the AO. Year-to-year changes in ice volume were inversely correlated with the intervening JFM AO index

resulting in longer-term volume changes that tended to parallel the AO's quasi-decadal phases. During the 1980s, when the AO was in a negative phase, average mid-winter SIT increased 7.6 cm $yr^{-1}$ throughout most of the Arctic and ice volume increased by approximately 2500 $km^3$. In 1989 the AO shifted to a pronounced positive phase and average SIT decreased through 1996 Arctic-wide by -6.1 cm $yr^{-1}$ with a concurrent volume loss of almost 4000 $km^3$. After 1996 the AO was variably neutral and average SIT modestly increased 2.1 cm $yr^{-1}$ (mostly in the central Arctic), but a corresponding volume increase was notably absent.

The modest thickening of sea ice in the high Arctic during 1996–2002 appears to have preserved perennial ice volume despite its declining extent. Nevertheless, thickening cannot compensate volume indefinitely if ice extent continues to decline. While the recent thickening may be in response to the AO's more neutral state, resilience for returning ice conditions to a prior regime is presently challenged by anomalously warm thermal forcing at the Arctic periphery. Future disposition of the thermal encroachment will play a determinant role in resolving the presently unstable relationship between thickness, volume, and the declining extent of the Arctic's perennial ice.

**Acknowledgements**

This paper is dedicated to the memory of its senior author, Professor Gennady I. Belchansky, who passed away during its revision. The study was carried out with support from the International Arctic Research Center, University of Alaska Fairbanks, and the USGS Global Change Research Program. We acknowledge NSIDC for providing ice concentration, ice motion, and submarine profile data, and R. E. Moritz for the North Pole Environmental Observatory

sonar data. We also thank S.-I. Akasofu, J. E. Walsh, I. Polyakov, and the anonymous reviewers for helping improve the scope, content and presentation of this paper.

REFERENCES


Belchansky, G. I., D. C. Douglas, and N. G. Platonov, 2004a: Duration of the Arctic sea ice melt season: regional and interannual variability, 1979–2001. *J. Climate,* **17**, 67–80.

——, ——, I. V. Alpatsky, and N. G. Platonov, 2004b: Spatial and temporal multiyear sea ice distributions in the Arctic: A neural network analysis of SSM/I data, 1988–2001. *J. Geophys. Res.*, **109**, C10017, doi:10.1029/2004JC002388.

——, ——, and N. G. Platonov, 2005a: Spatial and temporal variations in the age structure of Arctic sea ice. *Geophys. Res. Lett,* **32**, L18504, doi:10.1029/2005GL023976.

——, ——, V. A. Eremeev, and N. G. Platonov, 2005b: Variations in the Arctic's multiyear sea ice cover: A neural network analysis of SMMR-SSM/I data, 1979–2004. *Geophys. Res. Lett.,* **32**, L09605, doi:10.1029/2005GL022395.

Bishop, C. M., 1995: *Neural networks for pattern recognition*. Oxford University Press, 482 pp.

Bitz, C. M., and G. H. Roe, 2004: A mechanism for the high rate of sea ice thinning in the Arctic Ocean. *J. Climate,* **15**, 3623–3632.

Boyd, T. J., M. Steele, R. D. Muench, and J. T. Gunn, 2002: Partial recovery of the Arctic Ocean halocline. *Geophys. Res. Lett,*. **29**, 1657, doi:10.1029/2001GL014047.

Bourke, R. H., and R. P. Garret, 1987: Sea ice thickness distribution in the Arctic Ocean. *Cold Regions Sci and Tech.*, **13**, 259–280.

Castillo, E., O. Fontenla-Romero, A. A. Betanzos, and B. Guijarro-Berdi˜nas, 2002: A global optimum approach for one-layer neural networks. *Neural Computation*, **14**, 1429–1449.

Comiso, J., 1999: Bootstrap sea ice concentration for NIMBUS-7 SMMR and DMSP SSM/I. National Snow and Ice Data Center, digital media and CD-ROM, updated 2004. [Available online at http://nsidc.org/data/nsidc-0116.html.]

——, 2002: A rapidly declining perennial sea ice cover in the Arctic. *Geophys. Res. Lett.,* **29**, 1956, doi:10.1029/2002GL015650.

——, 2003: Warming trends in the Arctic from clear sky satellite observations. *J. Climate*, **16**, 3498–3510.

——, J. Yang, S. Honjo, and R. A. Krishfield, 2003: Detection of change in the Arctic using satellite and in situ data. *J. Geophys. Res.,* **108**, 3384, doi:10.1029/2002JC001347.

Curry, J. A., J. L. Schramm, A. Alam, R. Reeder, and T. E. Arbetter, 2002: Evaluation of data sets used to force sea ice models in the Arctic Ocean. *J. Geophys. Res.,* **107**, 8027, doi: 10.1029/2000JC000466.

Deser, C., J. E. Walsh, and M. S. Timlin, 2000: Arctic sea ice variability in the context of recent atmospheric circulation trends. *J. Climate,* **13**, 617–633.

——, M. Holland, G. Reverdin, and M. Timlin, 2002: Decadal variations in Labrador Sea ice cover and North Atlantic sea surface temperatures. *J. Geophys. Res.*, **107**, 3035, doi:10.1029/2000JC000683.

Eicken, H., W. B. Tucker, and D. K. Perovich, 2001: Indirect measurements of the mass balance of summer Arctic sea ice with an electromagnetic induction technique. *Ann. Glaciol.,* **33**, 194–200.

Fichefet, T., H. Goosse, and M. A. M. Magueda, 2003: A hindcast simulation of Arctic and Antarctic sea ice variability, 1955–2001. *Polar Res.,* **22**, 91–98.

Fowler, C., 2003: Polar Pathfinder daily 25 km EASE-grid sea ice motion vectors. National Snow and Ice Data Center, digital media. [Available online at http://nsidc.org/data/nsidc-0116.html.]

Francis, J. A., and E. Hunter, 2006: New insight into the disappearing Arctic sea ice. *EOS, Trans. Amer. Geophys. Union*, **87**, 509–511.

Haas, C., 2004: Late-summer sea ice thickness variability in the Arctic Transpolar Drift 1991-2001 derived from ground-based electromagnetic sounding. *Geophys. Res. Lett.,* **31**, 9402, doi:10.1029/2003GL019394.

——, and H. Eicken, 2001: Internannual variability of summer sea ice thickness in the Siberian and Central Arctic under different atmospheric circulation regimes. *J. Geophys. Res.,* **106**, 4449–4462.

Hansen, J., M. Sato, R. Ruedy, K. Lo, D. W. Lea, and M. Medina-Elizade, 2006: Global temperature change. *Proc. Natl. Acad. Sci. USA,* **103**, 14 288–14 293.

Hilmer, M., and P. Lemke, 2000: On the decrease of arctic sea ice volume. *Geophys. Res. Lett.,* **27**, 3751–3754.

Holland, M. M., and C. M. Bitz, 2003: Polar amplification of climate change in coupled models. *Climate Dyn.,* **21**, 221–232.

——, ——, E. C. Hunke, W. H. Lipscomb, and J. L. Schramm, 2006: Influence of the sea ice thickness distribution on polar climate in CCSM3. *J. Climate,* **19**, 2398–2414.

Holloway, G., and T. Sou, 2002: Has Arctic sea ice rapidly thinned? *J. Climate,* **15**, 1691–1701.

Johannessen, O. M., and others, 2004: Arctic Climate change: Observed and modeled temperature and sea ice variability. *Tellus Ser. A,* **56**, 1–18.

Karcher, M. J., R. Gerdes, F. Kauker, and C. Köberle, 2003: Arctic warming: Evolution and spreading of the 1990s warm event in the Nordic seas and the Arctic Ocean. *J. Geophys. Res.*, **108**, 3034, doi:10.1029/2001JC001265.

Köberle, C., and R. Gerdes, 2003: Mechanisms determining the variability of arctic sea ice conditions and export. *J. Climate,* **16**, 2843–2858.

Kwok, R., and D. A. Rothrock, 1999: Variability of Fram Strait ice flux and North Atlantic Oscillation. *J. Geophys. Res.*, **104**, 5177–5189.

——, and G. F. Cunningham, 2002: Seasonal ice area and volume production of the Arctic Ocean: November 1996 through April 1997. *J. Geophys. Res.,* **107**, 8038, doi:10.1029/2000JC000469.

Laxon, S., N. Peacock, and D. Smith, 2003: High inter annual variability of sea ice thickness in the Arctic region. *Nature*, **425**, 947–950.

Lindsay, R. W., and J. Zhang, 2005: The thinning of arctic sea ice, 1988–2003: Have we passed a tipping point? *J. Climate,* **18**, 4879–4894.

Løvås, S. M., and O. W. Brude, 1999: INSROP GIS – software and database, CD-ROM. Fridtjof Nansen Institute and Central Marine Research and Design Institute, PO Box 326, 1326 Lysaker, Norway.

Melling, H., 2001: Is the extent or thickness of Arctic sea ice declining? The State of the Arctic Cryosphere During the Extreme Warm Summer of 1998. Vol. II(11), CCAF Final Report. [Available online at http://www.socc.ca/summer/ftp/ftp.html.]

——, D. A. Riedel, and Z. Gedalof, 2005: Trends in the draft and extent of seasonal pack ice, Canadian Beaufort Sea. *Geophys. Res. Lett.,* **32**, L24501, doi:10.1029/2005GL024483.

Miller P. A., S. W. Laxon, D. L. Feltham, and D. J. Cresswell, 2006: Optimization of a sea ice model using basinwide observations of Arctic sea ice thickness, extent, and velocity. *J. Climate,* **19**, 1089–1106

NSIDC, 1998, updated 2006: Submarine upward looking sonar ice draft profile data and statistics. National Snow and Ice Data Center, digital media. [Available online at http://nsidc.org/data/g01360.html.]

——, 2004: Morphometric characteristics of ice and snow in the Arctic Basin: aircraft landing observations from the Former Soviet Union, 1928–1989. Compiled by I. P. Romanov. National Snow and Ice Data Center, digital media. [Available online at http://nsidc.org/data/g02140.html].

——, cited 2006: Arctic sea ice shrinks as temperatures rise. [Available online at http://nsidc.org/news/press/2006_seaiceminimum/20061003_pressrelease.html.

Overland, J. E., and M. Wang, 2005: The Arctic climate paradox: The recent decrease of the Arctic Oscillation. *Geophys. Res. Lett.,* **32**, L06701, doi:10.1029/2004GL021752.

Parkinson, C. L., and D. J. Cavalieri, 2002: A 21 year record of Arctic sea-ice extents and their regional, seasonal and monthly variability and trends. *Ann. Glaciol.,* **34**, 441–446.

——, D. Rind, R. J. Healy, D. J. Martinson, 2001: The impact of sea ice concentration accuracies on climate model simulations with the GISS GCM. *J. Climate,* **14**, 2606–2623.

Polyakov, I. V., and M. A. Johnson, 2000: Arctic decadal and interdecadal variability. *Geophys. Res. Lett.*, **27**, 4097–4100.

——, S.-I. Akasofu, U. Bhatt, R. Colony, M. Ikeda, A. Makshtas, C. Swingley, D. Walsh, and J. E. Walsh, 2002: Trends and variations in the Arctic climate system. *EOS, Trans. Amer. Geophys. Union,* **83**, 547–548.

——, and others, 2005: One more step toward a warmer Arctic. *Geophys. Res. Lett*., **32**, L17605, doi:10.1029/2005GL023740.

Riedmiller M., and H. Braun, 1993: A direct adaptive method for faster backpropagation learning: The RPROP algorithm. *Proc. IEEE Intl. Conf. on Neural Networks*, San Francisco, CA, USA, H. Ruspini, Ed., 586–591.

Rigor, I. G., R. L. Colony, and S. Martin, 2000: Variations in surface air temperature observations in the Arctic, 1979–97. *J. Climate,* **13**, 896–914.

——, J. M. Wallace, and R. L. Colony, 2002: Response of sea ice to the Arctic Oscillation. *J. Climate,* **15**, 2648–2663.

——, and ——, 2004: Variation in the age of Arctic sea-ice and summer sea-ice extent. *Geophys. Res. Lett.,* **31**, L09401, doi:10.1029/2004GL019492.

Rind, D., R. Healy, C. Parkinson, and D. Martinson, 1995: The role of sea ice in 2 × $CO_2$ climate model sensitivity. Part I: The total influence of sea ice thickness and extent. *J. Climate,* **8**, 449–463.

——, M. Chandler, J. Lerner, D. G. Martinson, and X. Yuan, 2001: Climate response to basin-specific changes in latitudinal temperature gradients and implications for sea ice variability. *J. Geophys. Res.*, **106**, 20 161–20 173.

Rothrock, D. A., and J. Zhang, 2005: Arctic Ocean sea ice volume: What explains its recent depletion? *J. Geophys. Res.*, **110**, C01002, doi:10,1029/2004JC002282.

——, Y. Yu, and G. A. Maykut, 1999: Thinning of the Arctic sea-ice cover. *Geophys. Res. Lett.,* **26**, 3469–3472.

——, J. Zhang, and Y. Yu, 2003: The Arctic ice thickness anomaly of the 1990s: a consistent view from observations and models. *J. Geophys. Res.*, **108**, 3083, doi:10,1029/2001JC001208.

Santer, B. D., T. M. L. Wigley, J. S. Boyle, D. J. Gaffen, J. J. Hnilo, D. Nychka, D. E. Parker, and K. E. Taylor, 2000: Statistical significance of trends and trend differences in layer-average atmospheric temperature time series. *J. Geophys. Res.*, **105**, 7337–7356.

Serreze, M. C., and J. A. Francis, 2006: The arctic amplification debate. *Climatic Change,* **76**, 241–264.

Shindell, D. T., R. L. Miller, G. A. Schmidt, and L. Pandolfo, 1999: Simulation of recent northern winter climate trends by greenhouse-gas forcing. *Nature*, **399**, 452–455.

Steele, M., W. Ermold, S. Häkkinen, D. Holland, G. Holloway, M. Karcher, F. Kauker, W. Maslowski, N. Steiner, and J. Zhang, 2001: Adrift in the Beaufort Gyre: a model intercomparison, *Geophys. Res. Lett.*, **28**, 2935–2938.

Stroeve, J. C., M. C. Serreze, F. Fetterer, T. Arbetter, W. Meier, J. Maslanik, and K. Knowles, 2005: Tracking the Arctic's shrinking ice cover: Another extreme September minimum in 2004. *Geophys. Res. Lett.,* **32**, L04501, doi:10.1029/2004GL021810.

——, T. Markus, W. Meier, and J. Miller, 2006: Recent changes in the Arctic melt meason. *Ann. Glaciol*., **44**, in press.

Thompson, D. W. J., and J. M. Wallace, 1998: The Arctic Oscillation signature in the wintertime geopotential height and temperature fields. *Geophys. Res. Lett.,* **25**, 1297–1300.

Thorndike, A. S., 1992: A toy model linking atmospheric thermal radiation and sea-ice growth. *J. Geophys. Res.*, **97**, 9401–9410.

Vinje, T., N. Nordlund, and A. Kvambekk, 1998: Monitoring ice thickness in Fram Strait. *J. Geophys. Res.,* **103**, 10 437–10 449.

Walsh, J. E., V. M. Kattsov, W. L. Chapman, V. Govorkova, and T. Pavlova, 2002: Comparison of Arctic climate simulations in uncoupled and coupled global climate models. *J. Climate,* **15**, 1429–1446.

Widell, K., S. Østerhus, and T. Gammelsrød, 2003: Sea ice velocity in the Fram Strait monitored by moored instruments. *Geophys. Res. Lett.,* **30**, 1982, doi:10.1029/2003GL018119.

Winsor, P., 2001: Arctic sea ice thickness remained constant during the 1990. *Geophys. Res. Lett.,* **28**, 1039–1041.

Witte, H., and E. Fahrbach, 2005: AWI moored ULS data, Greenland Sea and Fram Strait, 1991–2002. National Snow and Ice Data Center, digital media. [Available online at http://nsidc.org/data/g02139.html].

Woodgate, R. A., K. Aagaard, and T.J. Weingartner, 2006: Interannual changes in the Bering Strait fluxes of volume, heat and freshwater between 1991 and 2004. *Geophys. Res. Lett.*, **33**, L15609, doi:10.1029/2006GL026931.

Yu, Y., G. A. Maykut, and D. A. Rothrock, 2004: Changes in the thickness distribution of Arctic sea ice between 1958–1970 and 1993–1997. *J. Geophys. Res.,* **109**, C08004, doi:10.1029/2003JC001982.

Zhang, J., D. A. Rothrock, and M. Steele, 1998: Warming of the Arctic Ocean by a strengthened Atlantic inflow: model results. *Geophys. Res. Lett.,* **25**, 1745–1748.

——, ——, and ——, 2000: Recent changes in the Arctic sea ice: the interplay between ice dynamics and thermodynamics, *J. Climate*, **13**, 3099–3114

——, J., D. R. Thomas, D. A. Rothrock, R. W. Lindsay, Y. Yu, and R. Kwok, 2003: Assimilation of ice motion observation and comparisons with submarine ice thickness data. *J. Geophys. Res.,* **108**, C63170, doi:10.1029/2001JC001041.

Fig. 1. (a) Annual, (b) seasonal and (c) latitudinal averages (±1 sd) of the learning data SIT observations (n = 3064 pixels total) compared to their corresponding neural network estimates, and (d-f) analogous comparisons with independent SULS testing data (n = 844 pixels total). Asterisks along the top edge of figures d–f are positioned above comparisons with n ≤35 pixels.

Fig. 2. (a) January 1982–2003 sea ice thickness distributions; standard deviation, slope, and mean, and (b) January sea ice thickness slope during 1982–88, 1988–96, and 1996–2003.

Fig. 3. (a) Monthly sea ice thickness time series within a region of persistent perennial ice in the Arctic Ocean, and (b) seasonal oscillation of average (± 1 sd) monthly sea ice thickness in the same region.

Fig. 4. Monthly NN SIT time-series within a 100-km radius of the North Pole (black line) compared to the mean, median, and mode of intersecting SULS transects and a short time-series of freeboard-adjusted upward-looking sonar measurements from the North Pole Environmental Observatory. For comparison, freeboard-adjusted SULS SIT estimates are shown for the North Pole region from Rothrock et al. (1999, Table 2) and Yu et al. (2004, Fig. 3).

Fig. 5. (a) Monthly sea ice volume changes within the Arctic Ocean (blue) and the monthly amount of volume change due to ice flux across the Arctic Ocean boundary (red). (b) Beginning January 1982, the cumulative ice volume change within the Arctic Ocean (blue; with 36-month running average) and cumulative ice volume flux across the Arctic Ocean boundary (red).

Fig. 6. Month-to-month ice volume changes within the Arctic Ocean for months with significant linear slope. Plotted values are the within-year volume change from the previous month to the labeled month.

Fig. 7. Correspondence between average SIT and total volume (>65° N) at the time of (a) the winter volume maximum (March or April), and (b) the summer volume minimum (August or September). (c) Time series of the summer volume minimum and average thickness, highlighting the decoupled thickness-volume relationship after 1996.

Fig. 8. Relationship between year-to-year changes in (a) minimum and (b) maximum sea ice volume above 65° N and the intervening JFM AO index. Solid lines are linear slopes for all years 1982–2002 (dots); broken lines isolate the slopes for 1996–2002 (squares).

Fig. 9. Correlations (Pearson product-moment) between accumulated sums of the JFM AO over an increasing number of prior years and the annual minimum ice volume (solid) and the annual change in minimum ice volume (open) above 65° N. Correlations are significant ($S > 99\%$) for ice volume when $\rho < -0.52$ (n = 21), and for ice volume change when $\rho < -0.55$ (n = 20).

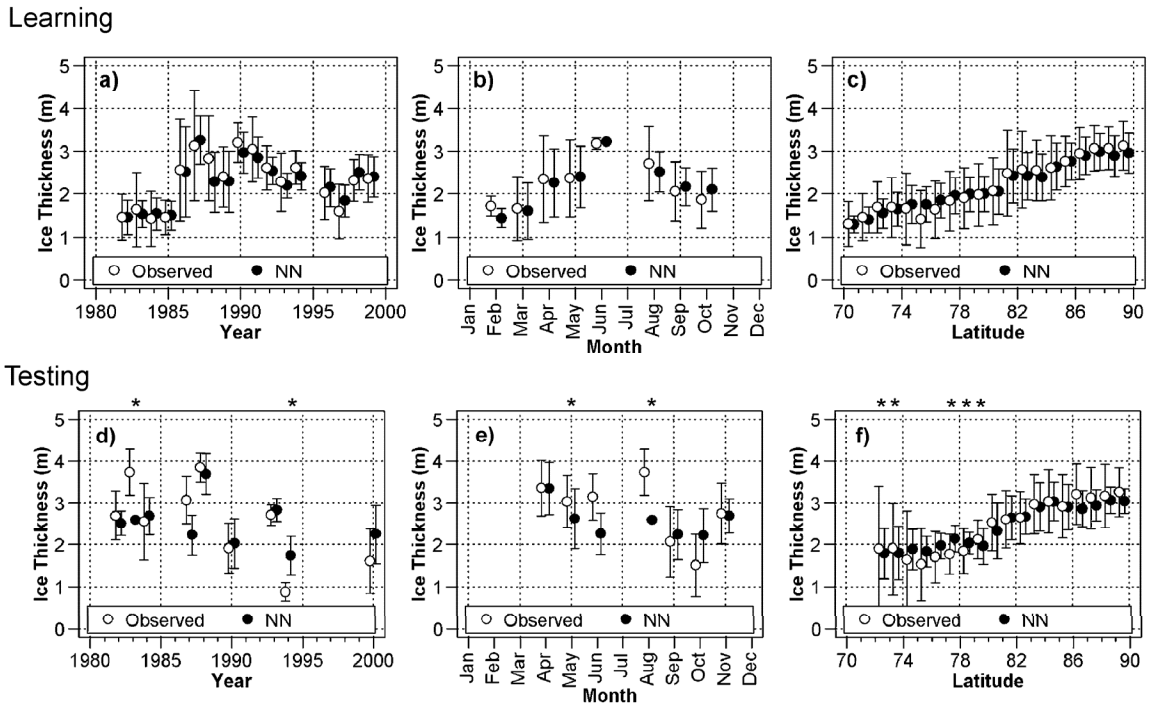


Fig. 1. (a) Annual, (b) seasonal and (c) latitudinal averages (±1 sd) of the learning data SIT observations (n = 3064 pixels total) compared to their corresponding neural network estimates, and (d-f) analogous comparisons with independent SULS testing data (n = 844 pixels total). Asterisks along the top edge of figures d–f are positioned above comparisons with n ≤35 pixels.

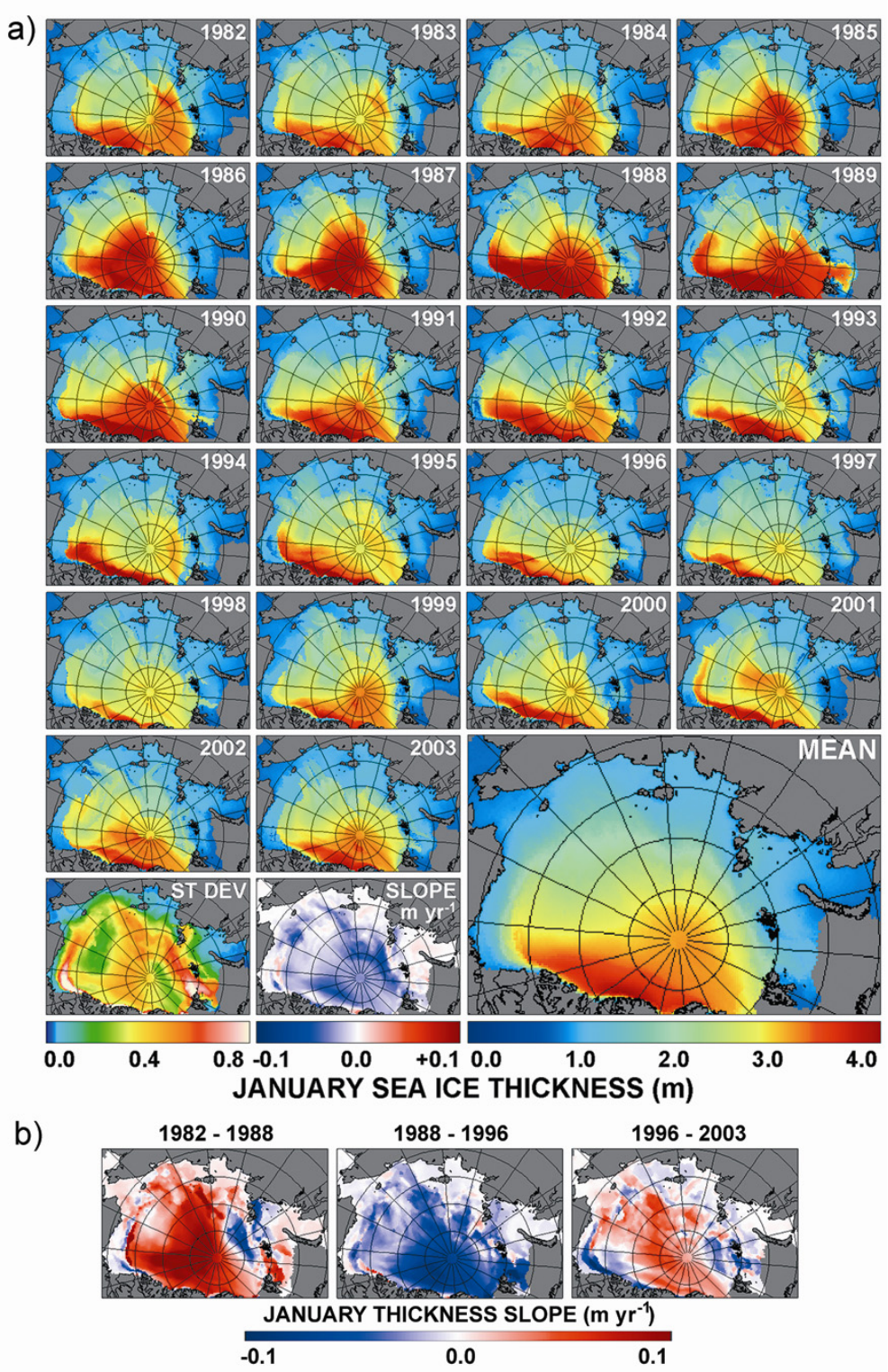


Fig. 2. (a) January 1982–2003 sea ice thickness distributions; variance, slope, and mean, and (b) January sea ice thickness slope during 1982–88, 1988–96, and 1996–2003.

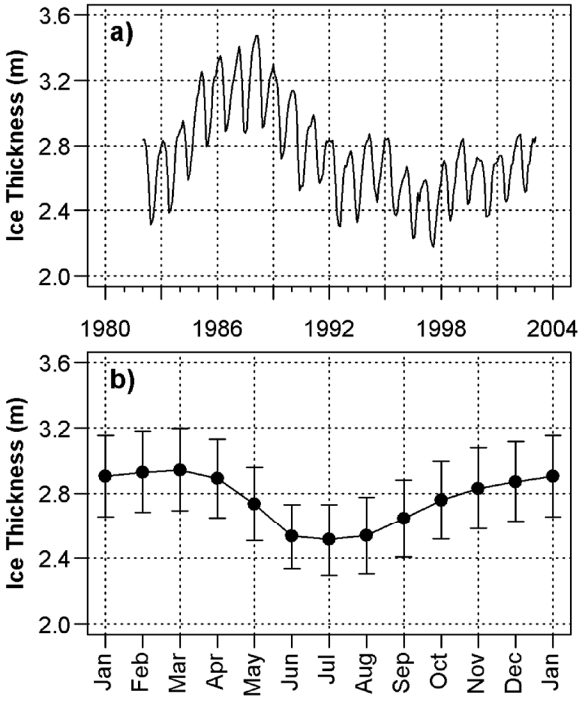


Fig. 3. (a) Monthly sea ice thickness time series within a region of persistent perennial ice in the Arctic Ocean, and (b) seasonal oscillation of average (± 1 sd) monthly sea ice thickness in the same region.

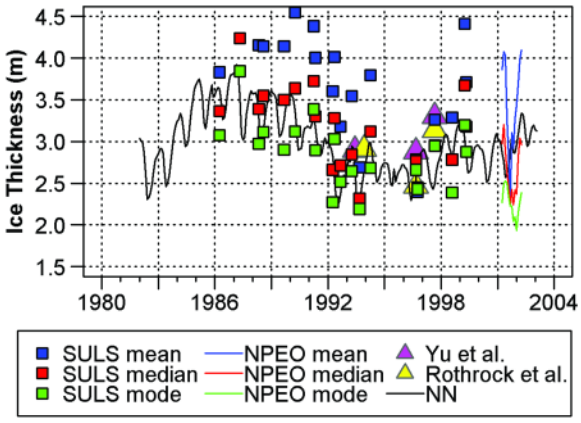


Fig. 4. Monthly NN SIT time-series within a 100-km radius of the North Pole (black line) compared to the mean, median, and mode of intersecting SULS transects and a short time-series of freeboard-adjusted upward-looking sonar measurements from the North Pole Environmental Observatory. For comparison, freeboard-adjusted SULS SIT estimates are shown for the North Pole region from Rothrock et al. (1999, Table 2) and Yu et al. (2004, Fig. 3).

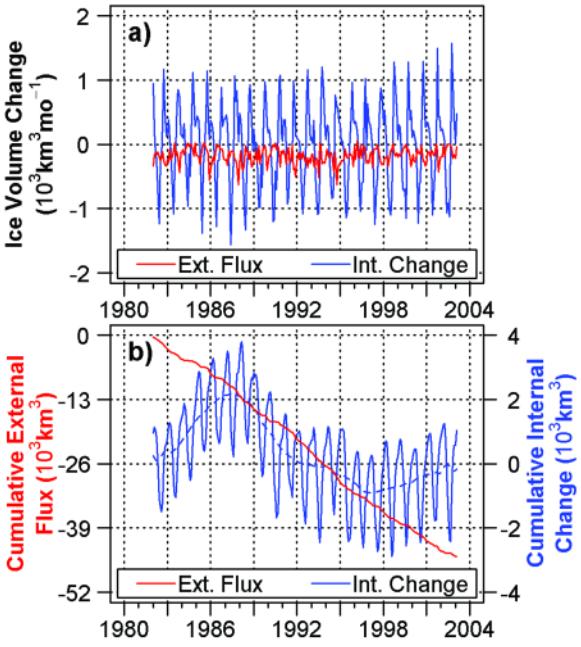


Fig. 5. (a) Monthly sea ice volume changes within the Arctic Ocean (blue) and the monthly amount of volume change due to ice flux across the Arctic Ocean boundary (red). (b) Beginning January 1982, the cumulative ice volume change within the Arctic Ocean (blue; with 36-month running average) and cumulative ice volume flux across the Arctic Ocean boundary (red).

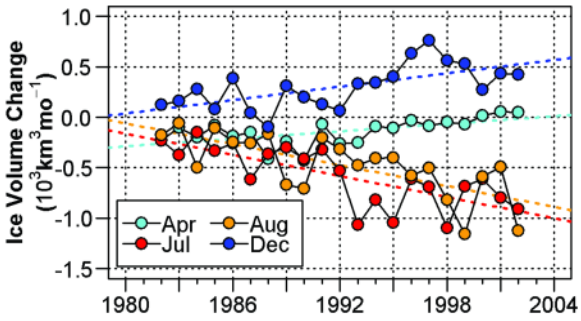


Fig. 6. Month-to-month ice volume changes within the Arctic Ocean for months with significant long-term linear slpoe. Plotted values are the within-year volume change from the previous month to the labeled month.

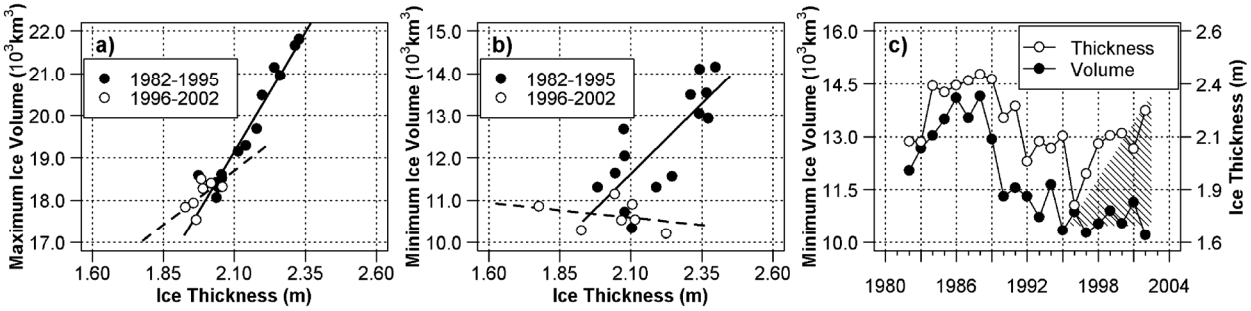


Fig. 7. Correspondence between average SIT and total volume (>65° N) at the time of (a) the winter volume maximum (March or April), and (b) the summer volume minimum (August or September). (c) Time series of the summer volume minimum and average thickness, highlighting the decoupled thickness-volume relationship after 1996.

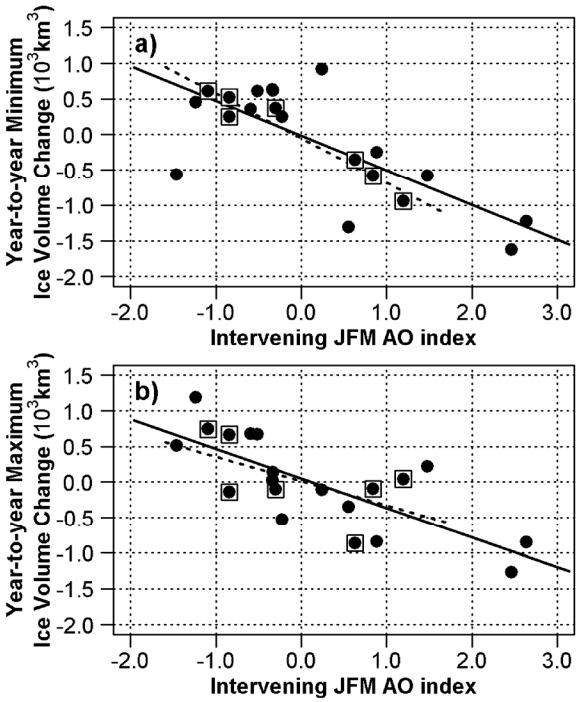


Fig. 8. Relationship between year-to-year changes in (a) minimum and (b) maximum sea ice volume above 65° N and the intervening JFM AO index. Solid lines are linear slopes for all years 1982–2002 (dots); broken lines isolate the slopes for 1996–2002 (squares).

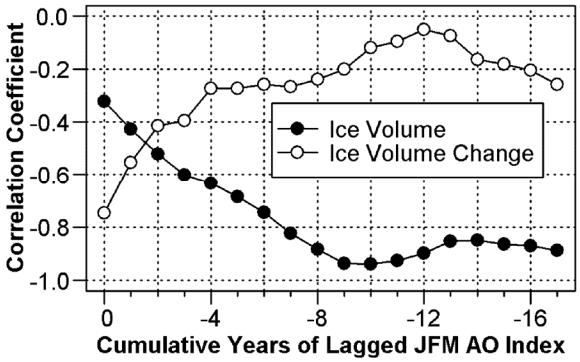


Fig. 9. Correlations (Pearson product-moment) between accumulated sums of the JFM AO over an increasing number of prior years and the annual minimum ice volume (solid) and the annual change in minimum ice volume (open) above 65° N. Correlations are significant ($S > 99\%$) for ice volume when $\rho < -0.52$ (n = 21), and for ice volume change when $\rho < -0.55$ (n = 20).

Table 1. Average discrepancies (m) between NN sea ice thickness estimates (X) and learning data, testing data, and several studies reporting in situ measurements and summaries (Y).

| | | General Locale | Mean Y-X | RMS | N |
|---|---|---|---|---|---|
| **Learning data (pixels)** | | | | | |
| SULS | | Arctic Ocean | -0.01 | 0.53 | 2157 |
| ALO | | Russian Arctic | 0.03 | 0.51 | 907 |
| SULS + ALO | | Arctic Ocean | 0.00 | 0.52 | 3064 |
| **Testing data (pixels)** | | | | | |
| SULS | | Arctic Ocean | 0.02 | 0.72 | 844 |
| **Pooled SULS data (regions)** | | | | | |
| *Rothrock et al.* (1999) | | Arctic Ocean | 0.11 | 0.42 | 15 |
| *Yu et al.* (2004) | | Arctic Ocean | -0.10 | 0.42 | 14 |
| **Field-site samples (pixels)** | | | | | |
| *Haas and Eicken* (2001)[1] | AWI | | | | |
| Drill-hole | | Eurasian Arctic | 0.18 | 0.90 | 147 |
| Electromagnetic | | Eurasian Arctic | -0.10 | 0.54 | 67 |
| CRREL[2] | | Beaufort Sea | 0.10 | 0.60 | 95 |
| **Monitoring stations (100-km radius)** | | | | | |
| *Moritz* (in prep)[3] | | North Pole | -0.24 | 0.43 | 13 |
| *Melling* (2001) | | SE Beaufort Sea | 0.37 | 1.07 | 72 |
| *Melling et al.* (2005) | | SE Beaufort Sea | 0.71 | 0.90 | 12 |
| *Vinje et al.* (1998) | | Fram Strait | 0.41 | 0.72 | 49 |
| *Witte and Fahrbach* (2005) | | Fram Strait | -0.51 | 0.92 | 117 |
| **Fram Strait transect (transect)** | | | | | |
| *Vinje et al.* (1998) | | Fram Strait | 0.02 | 0.60 | 68 |
| *Kwok and Rothrock* (1999) | | Fram Strait | -0.14 | 1.05 | 68 |
| **Map-to-map comparison (pixels)** | | | | | |
| *Løvås and Brude* (1999) | AARI | Arctic Ocean | 0.16 | 0.62 | 104878 |

Data sources:

[1] http://www.pangaea.de/
[2] http://www.crrel.usace.army.mil/sid/IMB/
[3] http://psc.apl.washington.edu/northpole/